Two-Photon Absorption Properties of Pyrene-based Dipolar D–π–A Fluorophores

Chuan-Zeng Wang,[a] Ruoyao Zhang,[b] Koya Sakaguchi,[a] Xing Feng,*[c] Xiaoqiang Yu,[b] Mark R.J. Elsegood,[d] Simon J. Teat,[e] Carl Redshaw,[f] and Takehiko Yamato*[a]

Abstract: Two-photon absorption (TPA) properties of pyrene-based derivatives are rare due to their limited controllable synthetic methodologies, but are in great demand given their potential practical application in practical photics and biological imaging. Herein, we present a set of pyrene-based dipolar donor–π–acceptor (D–π–A) fluorophores with a wide-range of colour tuning and large TPA cross-sections (up to 2200 GM at 780 nm) by regioselective substitution at the 1,3- and 6,8-positions under the perspective of theoretical analysis. The linear and nonlinear optical properties of these compounds have been studied. The near identical emission wavelength between the two-photon excited fluorescence (TPEF) and one-photon excited fluorescence (OPEF) indicated that they are generated from the same fluorescent excited state by either one- or two-photon excitations. With the exception of the strong donor [–$N(CH_3)_2$] appended fluorophore, the TPEF exhibited a large red-shift compared with the OPEF spectra due to the complicated working mechanisms in operation, including intramolecular charge transfer (ICT), and twisted intramolecular charge transfer (TICT). All fluorophores exhibit high two-photon cross sections (or two-photon brightness, $\delta\Phi$), especially for 1348 GM, which indicated that these materials can be used as colourants for probe and bioimaging applications.

Introduction

Light-emitting organic conjugated molecules with large two-photon absorption (TPA) cross-sections (δ) have attracted growing attention in recent decades, both at the theoretical and experimental level. This interest stems from their numerous potential applications in biologically-oriented research,[1] photodynamic therapy,[2] three-dimensional lithography/data storage,[3] and in the design of various other types of materials.[4] Within this context, developing rational strategies for the design and synthesis of molecules possessing large δ have led the trend in this field over recent years. Three basic structural motifs, namely dipolar,[5] quadrupolar,[6] and octupolar,[7] have been established, and are generalized by the construction of donor–acceptor–donor (D–A–D) type, donor–π-bridge–acceptor (D–π–A) type, donor–π-bridge–donor (D–π–D) type structures. Factors such as the geometrical parameters, including the extended π-conjugated system, the charge-transfer (CT) ability, and strength and position of electron-donating/electron-withdrawing groups influence the adoption of such motifs.[8] As well as the rapid progress on TPA, an active strategy for tuning the CT ability of prepared molecules with a desired TPA activity has been sought. In general, the high sensitivity of various vibrations to electronic density plays a crucial role on their TPA properties.[8c] Thus, a facile approach to prepare new charge-transfer molecules with tailored band gaps (ΔE_g) by introducing donor and acceptor groups was developed. Donors can provide a significant contribution to the high lying occupied molecular orbitals because they are prone to donate electrons. Acceptors on the other hand have an effect on the low lying unoccupied molecular orbitals because they are prone to accept electrons (Chart 1).[9] In the case of donor-acceptor (D-A) structures, the energy gap of the new materials can be significantly tuned compared with the parent components.

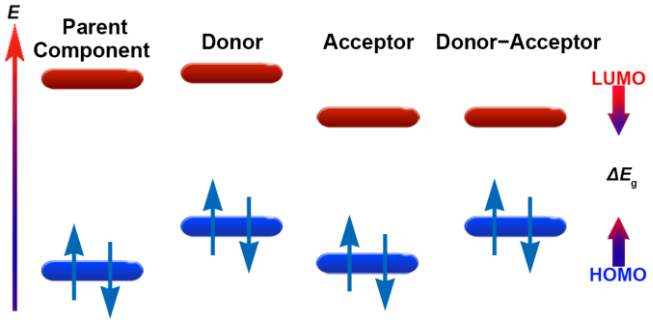

Chart 1. Schematic energy level diagram of D-π-A molecules.

One class of polycyclic aromatic hydrocarbons (PAHs) with a large π-conjugated core, excellent photoluminescence efficiency and deserving of particular attention is pyrene.[10] To date, pyrene-based fluorophores with TPA properties remain rare; examples include dipolar/quadrupolar molecules,[11] and multi-branch structural molecules.[12] Given this, the construction of pyrene-based D-π-A TPA materials with considerable δ values (even more than 1000 GM) is a promising strategy when pyrene is employed as the π-core. The previous studies have shown that donor/acceptor substituted pyrene-based derivatives can exhibit novel and tunable photophysical properties.[13] On the other hand, we also predicted that unsymmetrical D-π-A pyrene-

[a] C.-Z. Wang, K. Sakaguchi, Prof. T. Yamato
Department of Applied Chemistry, Faculty of Science and Engineering
Saga University
Honjo-machi 1, Saga 840-8502 Japan
E-mail: yamatot@cc.saga-u.ac.jp
[b] R.Y. Zhang, Prof. X.Q. Yu
Center of Bio & Micro/Nano Functional Materials
State Key Laboratory of Crystal Materials
Shandong University, Jinan 250100, China
[c] Dr. X. Feng
Faculty of Material and Energy Engineering
Guangdong University of Technology
Guangzhou 510006, China.
E-mail: hyxhn@sina.com
[d] Prof. M.R.J. Elsegood
Chemistry Department
Loughborough University
Loughborough, LE11 3TU, UK
[e] S.J. Teat
ALS, Berkeley Lab
1 Cyclotron Road, Berkeley, CA 94720, USA
[f] Prof. C. Redshaw
Department of Chemistry, School of Mathematics & Physical Sciences.
The University of Hull
Cottingham Road, Hull, Yorkshire HU6 7RX, UK

Supporting information for this article is given via a link at the end of the document.((Please delete this text if not appropriate))

based derivatives will possess efficient TPA properties. Taking account of the above considerations, by introducing different electron-donating/withdrawing substituents, a series of pyrene-based dipolar molecules, with tunable LUMO and HOMO levels and large δ value are reported (Scheme 1). Insight into the structure-property relationships of one-photon absorption and TPA of the five molecules reported herein was obtained by combining experimental and theoretical results, and evaluating the influence of donor and acceptor groups.

Results and Discussion

The synthetic procedure for **2** is outlined in Scheme 1, and was designed to gradually modulate the energy levels by changing the substituents. Thus, a set of pyrene-based dipolar molecules **2** were synthesized in high yield by the Pd-catalyzed coupling reaction of the precursor 1,3-diphenyl-6,8-dibromopyrene **1**.[13a] The structures and high purity were unambiguously confirmed by $^{1}H/^{13}C$ NMR spectroscopy, high-resolution mass spectrometry (HRMS) and X-ray crystallography. The detailed synthetic procedures and characterization data are given in the Supporting Information (ESI, Figs. S1−S10†). All compounds exhibited good solubility in common organic solvents and exhibited excellent thermal stability.

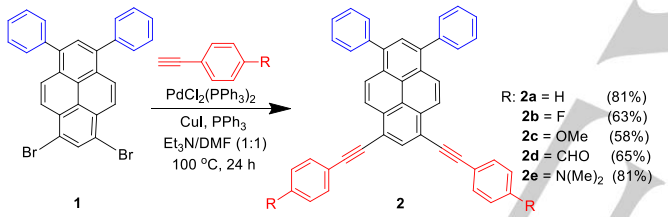

Scheme 1. Synthetic route to dipolar molecules **2**.

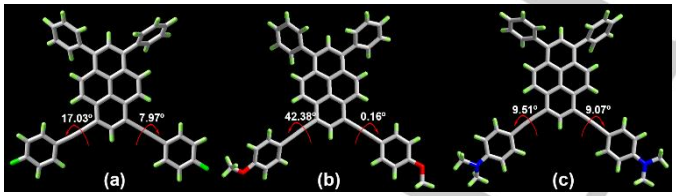

Figure 1. Crystal structures of **2b** (a), **2c** (b) and **2e** (c).

Single crystals of **2b**, **2c** and **2e** were obtained from chloroform/hexane mixtures by the slow solvent evaporation method, and were analyzed by single crystal X-ray diffraction crystallography using synchrotron radiation. As depicted in Figure 1, Table S1, and Figures S11-S13, in case of **2b** and **2e**, the two para-substituted rings are almost co-planar with the pyrene moiety, while the two phenyl groups are more substantially twisted in all three X-ray structures. The dihedral angles between the *para*-substituted rings and the pyrene core (C1 > C16) are 17.03(6)° (C39 > C44), 7.97(6)° (C31 > C36) for **2b**, and 9.51(9)° (C41 > C46), 9.07(9)° (C31 > C36) for **2e**. The twist angles between the pyrene core and the following phenyl groups are 47.18(4)° (C17 > C22), 62.78(3)° (C23 >C28) for **2b**, and 55.13(6)° (C17 > C22), 58.93(6)° (C23 > C28) for **2c**. It is worth noting that the NMe_2 *para* substituents of **2e** effectively weaken the π–π stacking interaction due to the twist angles between the C6 aromatic ring and the NMe_2 groups, 15.0(3)° (C31 > C36 and N1/C37/C38), 34.8(2)° (C41 > C46 and N2/C47/C48). For **2c**, there are four molecules of the pyrene plus one molecule of chloroform in the unsymmetrical unit. The twist angles (°) between the pyrene core and phenyl groups and C_6H_4 rings beyond the alkyne linkage are summarized in Table S2. In summary, the dihedral angles between the *para*-substituted rings beyond the alkyne linkage exhibit one shallow angle (range 0.16-8.61(19)° and one more twisted angle (range 42.38-49.55(11)°) with respect to the pyrene core, while the phenyl rings are all significantly twisted (range 41.23-58.54(14)°. A detailed investigation indicated that the molecular packing of **2b**, **2c**, and **2e** displayed marked differences. For **2b**, molecules pack in layers with zones of interdigitated phenyl groups and a separate zone of interdigitated F-substituted aromatic rings (Figure 2a). Molecules form off-set face-to-face $\pi\cdots\pi$ stacks with the centre of the pyrene overlaying the alkyne group C(29)/C(30) in a neighbouring molecule at a distance in the range 3.339–3.355 Å (depicted as orange dashed lines), and edge-to-face ArC–H$\cdots\pi$ interactions between the edge of the phenyl groups and the pyrene core at distances of 2.704 and 2.880 Å (Figure 2b bottom, depicted as blue dashed lines). For 2c, as shown in Figure 2c, 2d, the chloroform molecule either forms a C–H$\cdots\pi$ interaction with ring C(17) > C(22) or with a symmetry generated ring C(23B) > C(28B). Meanwhile, the molecules stack in slipped columns parallel to *a* with pyrene cores only just overlapping. Similar $\pi\cdots\pi$ stacks with the centre of the pyrene or C_6H_4 rings overlaying the alkyne group at a distance in the range

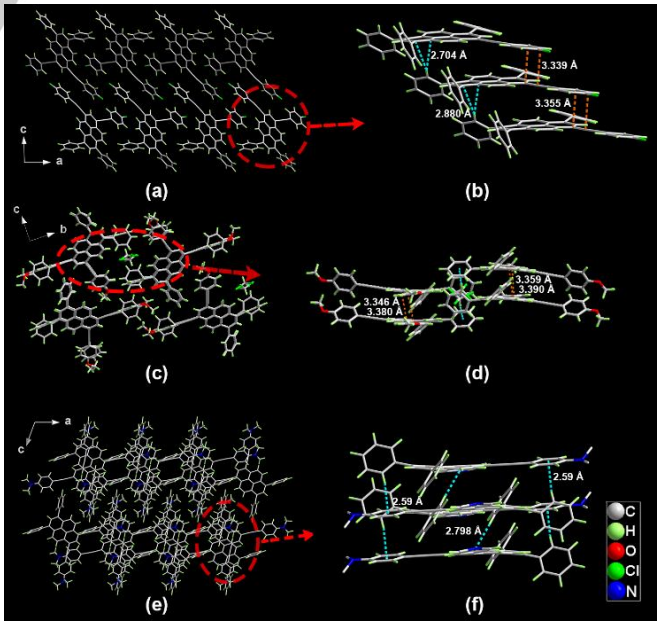

Figure 2. Crystal structures of **2b** (a) & (b), **2c** (c) & (d), and **2e** (e) & (f); Illustration of crystal packing and intermolecular interactions.

3.346–3.390 Å were observed. On the other hand, for **2e**, the more twisted conformations associated with the *para*-substituents can alleviate the intermolecular *π*−*π* stacking interactions to some degree, and instead they overlay with one of the alkyne groups C(39)/C(40) of a neighbouring molecule. This off-set stacking occurs parallel to *b*. The closest C···C interactions are *ca*. 3.42 Å. There are also rather distorted centro-symmetric pairs of ArC(24)–H(24)···*π* {centroid of ring C(41) > C(46)} interactions with a short distance of 2.59 Å (Figure 2f, blue dashed lines). These results demonstrate that compared with the F-substituted analog **2b**, the *π*−*π* stacking interactions between the NMe_2-substituted molecules are substantially weakened due to the bulky *para* substituent, which should favour tunable emission properties in solution with more substantially twisted structures.

Initially, density functional theory (DFT) calculations were performed to evaluate the energy levels of this type of dipolar molecule at the B3LYP/6-31G* level. As depicted in Figure 3, the energy gaps gradually reduce from **2a** to **2e**, which further indicated that this strategy to tune the LUMO and HOMO levels is an efficient process. Compared with the compound 1,3-diphenylpyrene (3.58 eV), compounds **2** exhibited distinctly lower energy gaps, which is due to the introduction of donor or acceptor groups at the 6-, and 8- positions. Compared with **2a**, the energy gaps of the other four compounds **2b**−**2e** also gradually reduce, which is associated with the donating- or withdrawing-electron ability of the substituents (**R**) at the *para*-position of arylethynyl. Specifically, relative to **2a** (**R** = **H**), **2b** (**R** = **F**) and **2c** (**R** = **OMe**), the substituent groups at the 6-, and 8-positions are weakly electron-withdrawing/donating substituents, respectively, and provide a certain degree of influence over the LUMOs and HOMOs. For compound **2d** (**R** = **CHO**), the terminal substituent is a strong electron-withdrawing group, and so it provided energetically enhanced LUMOs, which are mainly distributed over the pyrene core and arylethynyl substituents. On the contrary, the HOMOs of compound **2e** (**R** = **N(CH₃)₂**), with strong electron-donating substituents, are mostly localized on the pyrene core and arylethynyl substituents. This implies that the HOMOs and LUMOs are determined by the terminal substituents **R**.[14] Theoretical studies indicate that there are several effective strategies to improve the TPA cross-sections, such as highly delocalized conjugated system, increased intramolecular charge transfer character, and multi-branched molecular structures. Consequently, in our present systems, the extended conjugated D–*π*–A molecules with ICT character along the long axis were predicted that they possess TPA properties, especially for compounds **2d** and **2e**.

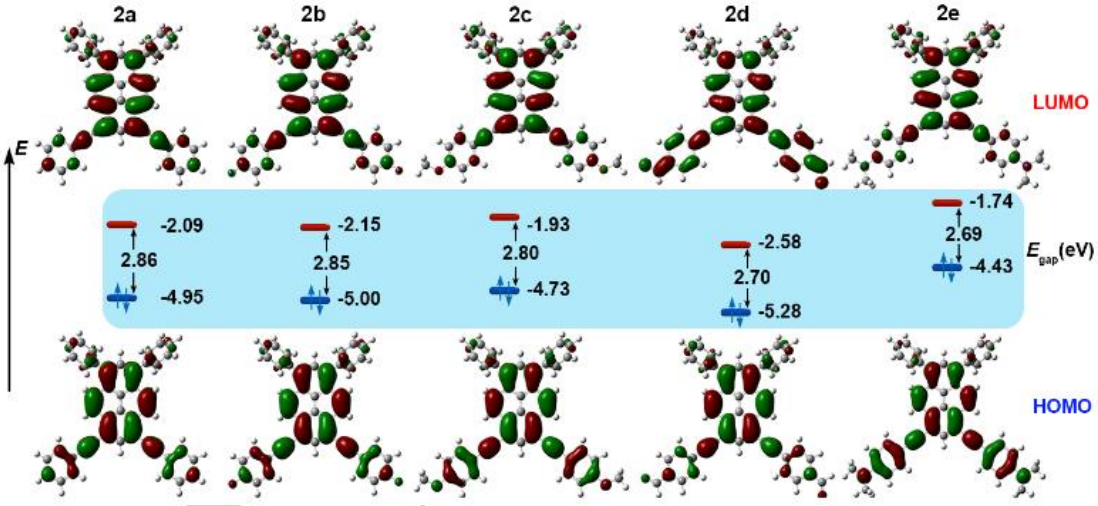

Figure 3. Frontier-molecular-orbital distributions and energy level diagram of **2a**−**e** by DFT calculations.

Further investigations of the UV-vis absorption and emission properties were performed for compounds **2** based on our preliminary theoretical guidance, and the key spectroscopic parameters are summarized in Table 1. As shown in Figure 4a, the absorption spectra of **2** in dichloromethane are distinctive but complicated, which is attributed to the D-*π*-A type molecular structures and the extended *π*-conjugated system. A gradual bathochromic shift was observed in the order **2a** ≈ **2b** < **2c** < **2d** < **2e**, indicating the increasing tendency of intramolecular charge transfer (ICT). On the other hand, the type of absorption profiles present obvious distinctions, especially for **2d** and **2e**, the more tuneable and sensitive absorption properties are mainly associated with the extent of ICT and twist intramolecular charge transfer (TICT). Specifically, for **2a**-**2c**, three sets of pronounced absorption bands were observed. Firstly, a short-wavelength band distributed in less than 250 nm which is mainly due to the *π*−*π** transitions of the phenyl groups and the pyrene core. Secondly, a long-wavelength band localized in the range of 409−434 nm with high molar absorption coefficients (53100−70100 cm^{-1} M^{-1}), and lastly an absorption band mainly

centered at 318–336 nm with higher values for the molar absorption coefficients (49600−82800 cm^{-1} M^{-1}). However, more obvious and complicated characteristic absorption bands were noted for **2d** and **2e**. In particular, new absorption bands at 367 nm with a low value of ε (39800 cm^{-1} M^{-1}) for **2d**, and at 388 nm with a low value of molar absorption coefficients (52300 cm^{-1} M^{-1}) for **2e** were observed, respectively. The results of the above mentioned results for compounds **2** indicate that their excited states possess significant charge transfer (CT) absorption associated with the withdrawing- or donating-electron peripheral unit at the 6,8-diarylethynyl terminal substituents in these D-π-A systems.

Table 1 Linear and nonlinear optical properties of compounds **2a**–**e**.

Compd	λ_{abs} [nm] sol[a] (ε [M^{-1} cm^{-1} L])	λ_{em} [nm] sol[a]	Φ_{fl} [%] Sol[a]	10^3 $\Delta\nu$ [cm^{-1}][b]	Φ_{fl} [%] Sol[c]	λ_{TPE}^{max} [nm][d]	δ_s[e] [GM]	$\delta_s \times \Phi_s$[f]
2a	318 (82800), 429 (70100)	453	77	1.24	85	459	202 (780 nm)	171
2b	318 (71300), 428 (60600)	452	76	1.24	85	456	172 (780 nm)	147
2c	325 (49800), 434 (53100)	458	78	1.21	85	461	73 (800 nm)	63
2d	256 (49800), 330 (48800) 367 (39800), 445 (53600)	485	75	1.85	93	506	1450 (780 nm)	1348
2e	255 (52600), 315 (50700) 388 (52300), 454 (58000)	532	80	3.23	29	657	2210 (780 nm)	641

[a] Measured in dichloromethane at room temperature. [b] Stokes-shift. [c] Measured in DMSO at room temperature. [d] Measured in DMSO at room temperature. [e] δ is two-photon absorption cross sections determined using fluorescein (Φ_{fl} = 0.95) as the standard,[15] ± 15%. [f] $\delta \times \Phi$ is two-photon action cross sections.

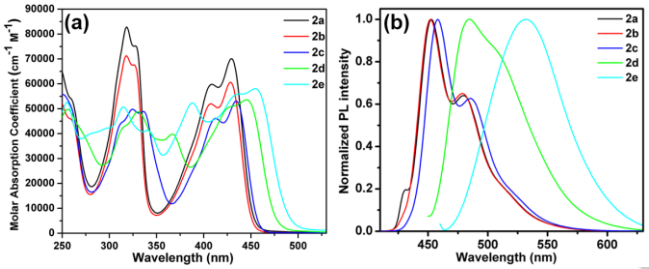

Figure 4. One-photon absorption (a) and emission (b) profiles for compounds **2** in CH_2Cl_2 solution.

In contrast, the fluorescence spectra of compounds **2** exhibit a clear and simple emission band, the emission maxima are in the range 452−532 nm in CH_2Cl_2 solution (c = 5 × 10^{-7} M) with a sequential bathochromic shift in the order **2a** ≈ **2b** < **2c** < **2d** < **2e** (Figure 4b). This is highly consistent with the energy gaps from the DFT calculation results; the energy gap (E_g) between the Franck-Condon and emitting state decreases in the same order. As expected, combined with the theoretical calculations, slight bathochromic shifts (< 5 nm) between **2a**–**c** were observed, while **2d**–**f** exhibited a distinct bathochromic shift (33−80 nm) compared with the former. To further elucidate the emission mechanism of this D-π-A system, solvatochromism was performed in solvents of different polarities (cyclohexane, CHX; 1,4-dioxane, DOA; tetrahydrofuran, THF; dichloromethane, DCM; and dimethyl formamide, DMF). The absorption properties of this set of compounds **2** displayed different sensitivities for the polarity. For compounds **2a**-**2d**, they present almost identical absorption spectra from cyclohexane to DMF (less than 4 nm red-shifts). On the other hand, for compound **2e**, a large red-shift (12 nm) and change of absorption bands were observed from cyclohexane to DMF, which is ascribed to the TICT of twist geometry. As shown in Figure 5 and the Supporting Information (Figure S15), the fluorescence spectra of this set of compounds are sensitive toward to the solvent polarity, especially for **2e**, where the emission maximum displayed a remarkable red-shift on increasing the solvent polarity (cyclohexane 470 nm, DMF 582 nm). And the weak emission band as a shoulder at long wavelength indicated that there may be a TICT state in cyclohexane, with the increase of solvent polarity, the CT emission and local emission are overlap. The relationship between the Stokes shifts in various solvents and the Lippert−Mataga equation was investigated,[16] and a nearly linear correlation between these two factors was evident (Figure 5b). The slopes of the linear fits for compounds **2a**−**e** are 16, 14, 17, 80 and 569 cm^{-1}, respectively, which indicates an increasing trend for the charge transfer.[17] Concentration dependent experiments were carried out in CH_2Cl_2 solution successively, and the emission properties of these compounds are consistent with the X-ray structural information. Taking compound **2b** as an example, the emission spectra exhibited a wide peak at 452 nm with a shoulder at 478 nm in dilute solution, and the shoulder band has gradually become domination with increase of concentration, which results from the formation of excimer. The fluorescence quantum yields and emission decay profiles of the

compounds **2** are shown in Table 1. All compounds exhibit high quantum yields (≥ 0.75) and considerably short lifetimes (≤ 15 ns) at room temperature (Figure S17). The same prompt and delayed PL emissions readily reveals the emission state resulting from the lowest singlet excited state.[18]

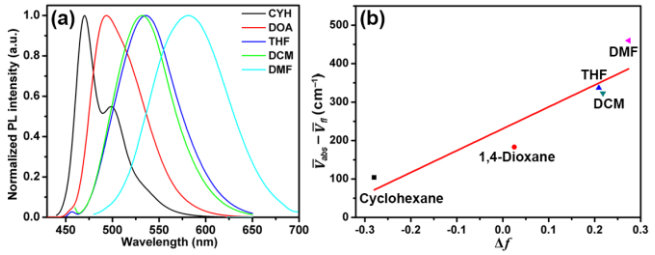

Figure 5. (a) Emission spectra of **2e** in cyclohexane, 1,4-dioxane, THF, DCM, and DMF at room temperature; (b) Lippert−Mataga plots for compound **2e**.

The two-photon absorption (TPA) spectra of the five compounds **2** were studied using a two-photon-excited fluorescence (TPEF) technique with a femtosecond pulsed laser source.[19]

TPA cross sections (δ) have been measured using the two-photon induced fluorescence method,[20] and thus the cross section can be calculated by means of Eq. (1):

$$\delta_s = \delta_r \frac{\phi_r c_r n_r F_s}{\phi_s c_s n_s F_r} \quad (1)$$

where the subscripts *s* and *r* refer to the sample and the reference materials, respectively. δ is the TPA cross section value, *c* is the concentration of the solution, Φ is the fluorescence quantum yield, *F* is the two-photon excited fluorescence integrated intensity, and *n* is the refractive index. δ_r is the two-photon absorption cross-section of fluorescein in sodium hydroxide aqueous solution (pH = 13.0) as the standard.[21]

The TPA spectra of a series of compounds **2** were performed in DMSO solution at 20 nm intervals from 780 to 900 nm by using a femtosecond pulsed laser source. The TPA spectra of compounds **2** are presented in Figure 6. Depending on the extended π-conjugation and intramolecular charge-transfer over the entire molecule, all the compounds displayed large TPA cross-sections δ_s, (δ, expressed in GM = 10^{-50} cm^4 · S · photon^{-1} · molecule^{-1}). The δ_s values, 202 GM for **2a** at 780 nm, 172 GM for **2b** at 780 nm, 73 GM for **2c** at 800 nm, 1450 GM for **2d** at 780 nm, 2210 GM for **2e** at 780 nm, are reasonable compared with other reported functionalized pyrene-based small molecules. Especially for **2d** (1450 GM) and **2e** (2210 GM), the δ_s values are large by comparison with other small pyrene-based molecules reported to-date,[11] indicating that the extended π-conjugation and increased ICT behaviour are favourable features to access high-efficiency organic molecules with large δ values. Moreover, the performance of two-photon active fluorescent molecules is generally evaluated according to the value of the two-photon action cross sections ($\delta \times \Phi$), which are an indicator of the brightness of the emission process. In this type of molecule, the $\delta\Phi$ values for **2d** (1348 GM) and **2e** (641 GM) are distinctly large compared with the values for other pyrene-based TP active fluorescents. Although the trend in the δ_s values are not exact consistent with the abilities of intramolecular charge transfer from **2a** to **2e**, as one of the critical factors, theoretical results indicated that strong electron-withdrawing (**2d**) and electron-donating (**2e**) groups play a leading role in TPA properties. This result implies that pyrene as an efficient π-center may serve as a promising two-photon imaging material for various applications.[22]

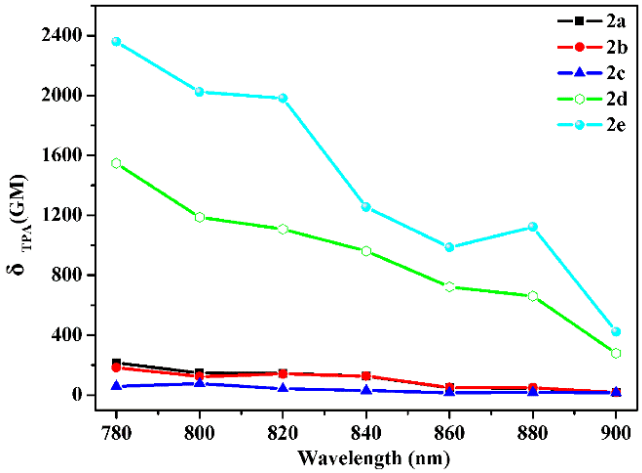

Figure 6. Two-photon excitation spectra of **2a−e** in DMSO. Error limit: 15%.

Apart from TPA properties, the two-photon excited fluorescence (TPEF) of **2** was also studied under the same experimental conditions (λ_{ex} = 780 nm). As shown in Figure 7 and Table 1, the spectral profiles for the TPEF are basically identical to the one-photon excited fluorescence (OPEF) except for **2e**. The similarities between the TPEF and OPEF indicated that they would finally relax to the same fluorescent excited state by either one- or two-photon excitations. Thus, for compounds **2a−d**, it seems to be impartial to the influence of the TPEF and OPEF properties except for a slight red-shift (no more than 5 nm). On the other hand, the different spectral selection rules for TPA and one-photon absorption (OPA) processes can lead to different excited states in these two cases.[23] For compound **2e**, a large red-shift (49 nm) was observed, and we assume that the distinction results from the reabsorption effect.[24] The effect occurs at high concentration; (10^{-5} mol/L for the measurement of TPEF, and 10^{-7} mol/L for the measurement of OPEF). Furthermore, such red-shifted emission spectra can be ascribed to the different emitting states accessed by one- or two-photon excitation.[25]

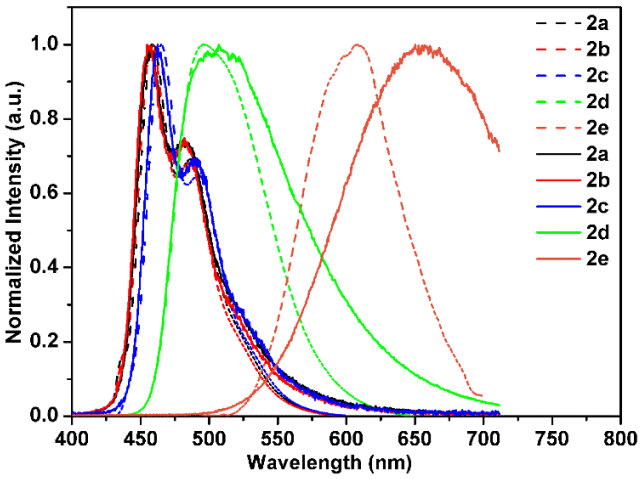

Figure 7. Normalized two-photon excited fluorescence spectra (solid line, λ_{ex} = 800 nm) of compounds **2** in DMSO solution. One-photon excited fluorescence spectra are shown for comparison (dashed line).

Presented here, the OPEF and TPEF properties combined with theoretical calculations indicate that D–*π*–A pyrene systems exhibit excellent tunability for the design of large TPA cross sections and two-photon action cross sections. This type of molecule is not only a promising OPEF activator, but also an efficient TPEF fluorophore.

Conclusions

In conclusion, we have demonstrated an efficient and facile strategy for the design and synthesis of D–*π*–A pyrene-based fluorophores with large TPA cross section, which benefit from theoretical guidance. A microscopic rule was employed to prepare a series of dipolar molecules with graded energy gaps. Aided by this method, the first example of small pyrene-based dipolar molecules with *δ* above 2200 GM is reported, which can be attributed to the strong electron-donating nature of the $-N(CH_3)_2$ groups present. The electron-withdrawing nature of the –CHO groups results in a dipolar molecule with high quantum yield (93%) and large TP action cross section (1348 GM). Such OPEF and TPEF properties indicate a promising application in two-photon imaging materials. More studies are necessary to understand the underlying mechanisms of this type of molecule, and further detailed investigations are aimed at developing such TPA fluorophores in our laboratory.

Experimental Section

General procedures

Synthetic routes for the five compounds **2** are shown in Scheme 1. All reactions were carried out under a dry N_2 atmosphere. Solvents were Guaranteed reagent (GR) for cyclohexane, 1,4-dioxane, tetrahydrofuran (THF), dichloromethane (CH_2Cl_2), dimethylformamide (DMF), and dimethyl sulfoxide (DMSO), and stored over molecular sieves. Other reagents were obtained commercially and used without further purification. Reactions were monitored using thin layer chromatography (TLC). Commercial TLC plates (Merck Co.) were developed and the spots were identified under UV light at 254 and 365 nm. Column chromatography was performed on silica gel 60 (0.063-0.200 mm). All melting points (Yanagimoto MP-S1) are uncorrected. $^1H/^{13}C$ NMR spectra were recorded on a Varian-400MR-vnmrs 400 with $SiMe_4$ as an internal reference. Mass spectra were obtained with a Nippon Denshi JMS-HX110A Ultrahigh Performance mass spectrometer at 75 eV using a direct-inlet system. UV/ Vis spectra were obtained with a Perkin–Elmer Lambda 19 UV/Vis/NIR spectrometer in various organic solvents. Fluorescence spectroscopic studies were performed in various organic solvents in a semimicro fluorescence cell (Hellma®, 104F-QS, 10 × 4 mm, 1400 µL) with a Varian Cary Eclipse spectrophotometer. Fluorescence quantum yields were measured using absolute methods.

Experimental details.

Synthesis of 1,3-diphenyl-6,8-diarylethynylpyrenes (2a–e)

A series of compounds **2a–e** were synthesized from 1,3-diphenyl-6,8-dibromopyrene **1**[13a] using the corresponding aryl alkyne by a Sonogashira coupling reaction.

1,3-Diphenyl-6,8-bis-(phenylethynyl)pyrene 2a

A mixture of 1,3-diphenyl-6,8-dibromopyrene **1** (102 mg, 0.2 mmol), phenylacetylene (82 mg, 0.8 mmol), $PdCl_2(PPh_3)_3$ (14 mg, 0.02 mmol), CuI (7.6 mg, 0.04 mmol), PPh_3 (5 mg, 0.02 mmol) was added to a degassed solution of Et_3N (5 mL) and DMF (5 mL). The resulting mixture was stirred at 100 °C for 24 h. After it was cooled to room temperature, the reaction was quenched with water. The mixture was extracted with CH_2Cl_2 (2 × 500 mL), the organic layer was washed with water (2 × 30 mL) and brine (30 mL), and then the solution was dried ($MgSO_4$), and evaporated. The residue was purified by column chromatography eluting with a 1:3 $CHCl_3$/hexane mixture to give **2a** as a organe solid (recrystallized from hexane:$CHCl_3$=4:1, yield: 95 mg, 81.2%); Mp 195–196°C; ^1H NMR (400 MHz, $CDCl_3$): δ_H = 7.41 (d, *J* = 7.3 Hz, 6H, Ar-*H*), 7.47–7.52 (m, 2H, Ar-*H*), 7.57 (t, *J* = 7.3 Hz, 4H, Ar-*H*), 7.68 (d, *J* = 6.3 Hz, 8H, Ar-*H*), 8.04 (s, 1H, pyrene-*H*), 8.35 (d, *J* = 9.4 Hz, 2H, pyrene-*H*), 8.45 (s, 1H, pyrene-*H*), 8.64 (d, *J* = 9.4 Hz, 2H, pyrene-*H*) ppm; ^{13}C NMR (100 MHz, $CDCl_3$): δ_C = 88.0, 95.4, 117.7, 123.4, 124.9, 125.1, 125.5, 127.0, 127.5, 128.2, 128.5, 128.5, 130.0, 130.6, 130.7, 131.7, 132.0, 133.4, 138.6, 140.7 ppm; FAB-MS: *m/z* calcd for $C_{44}H_{26}$ 554.2037 [M^+]; found 554.2035 [M^+].

A similar procedure using phenylacetylene, 4-fluorophenyl acetylene, 4-methoxyphenyl acetylene, 4-formylphenyl acetylene, was followed for the syntheses of **2b–e**.

1,3-Diphenyl-6,8-bis-(4'-fluorophenylethynyl)pyrene 2b was obtained as a yellow solid (recrystallized from hexane:$CHCl_3$=3:1, yield: 115 mg, 63.6%); Mp 263–264°C; ^1H NMR (400 MHz, $CDCl_3$): δ_H = 7.12 (t, *J* = 8.1 Hz, 4H, Ar-*H*), 7.47–7.52 (m, 2H, Ar-*H*), 7.57 (t, *J* = 7.0 Hz, 4H, Ar-*H*), 7.67 (t, *J* = 7.1 Hz, 8H, Ar-*H*), 8.05 (s, 1H, pyrene-*H*), 8.35 (d, *J* = 9.4 Hz, 2H, pyrene-*H*), 8.41 (s, 1H, pyrene-*H*), 8.60 (d, *J* = 9.4 Hz, 2H, pyrene-*H*) ppm; ^{13}C NMR (100 MHz, $CDCl_3$): δ_C = 87.7, 94.4, 110.1, 115.76, 116.0,

117.5, 119.5, 125.1, 125.4, 127.2, 127.6, 128.2, 128.5, 130.1, 130.7, 132.1, 133.3, 133.6, 133.6, 138.7, 140.7, 161.5 ppm; FAB-MS: *m/z* calcd for $C_{44}H_{24}F_2$ 590.1846 [M^+]; found 590.1844 [M^+].

1,3-Diphenyl-6,8-bis-(4'-methoxyphenylethynyl)pyrene 2c was obtained as a pale-yellow solid (recrystallized from hexane:CH_2Cl_2=2:1, yield: 107 mg, 58.2%); Mp 169–170°C; ^{1}H NMR (400 MHz, $CDCl_3$): δ_H = 3.87 (s, 6H, *Me*), 6.95 (d, *J* = 7.0 Hz, 4H, Ar-*H*), 7.47–7.52 (m, 2H, Ar-*H*), 7.57 (t, *J* = 7.3 Hz, 4H, Ar-*H*), 7.63 (d, *J* = 6.9 Hz, 4H, Ar-*H*), 7.68 (d, *J* = 7.8 Hz, 4H, Ar-*H*), 8.03 (s, 1H, pyrene-*H*), 8.33 (d, *J* = 9.4 Hz, 2H, pyrene-*H*), 8.41 (s, 1H, pyrene-*H*), 8.63 (d, *J* = 9.4 Hz, 2H, pyrene-*H*) ppm; ^{13}C NMR (100 MHz, $CDCl_3$): δ_C = 54.5, 85.9, 94.6, 113.3, 114.6, 117.1, 124.1, 124.2, 124.6, 125.8, 126.6, 127.3, 127.5, 129.0, 129.8, 130.7, 132.1, 132.3, 137.4, 139.8, 158.9 ppm; FAB-MS: *m/z* calcd for $C_{46}H_{30}O_2$ 614.2246 [M^+]; found 614.2248 [M^+].

1,3-Diphenyl-6,8-bis-(4'-formylphenylethynyl)pyrene 2d was obtained as an orange solid (recrystallized from hexane:$CHCl_3$=1:1, yield: 107 mg, 65.5%); Mp 177–178°C; ^{1}H NMR (400 MHz, $CDCl_3$): δ_H = 7.49–7.54 (m, 2H, Ar-*H*), 7.58 (t, *J* = 7.6 Hz, 4H, Ar-*H*), 7.68 (d, *J* = 8.0 Hz, 4H, Ar-*H*), 7.81 (d, *J* = 7.9 Hz, 4H, Ar-*H*), 7.92 (d, *J* = 7.6 Hz, 4H, Ar-*H*), 8.08 (s, 1H, pyrene-*H*), 8.39 (d, *J* = 9.4 Hz, 2H, pyrene-*H*), 8.46 (s, 1H, pyrene-*H*), 8.60 (d, *J* = 9.4 Hz, 2H, pyrene-*H*) ppm; ^{13}C NMR (100 MHz, $CDCl_3$): δ_C = 91.9, 94.6, 110.0, 116.7, 125.1, 127.7, 127.9, 128.0, 128.5, 129.5, 129.7, 130.2, 130.5, 130.7, 132.1, 132.7, 133.7, 135.6, 139.2, 140.4, 191.3 ppm; FAB-MS: *m/z* calcd for $C_{46}H_{26}O_2$ 610.1934 [M^+]; found 610.1933 [M^+].

1,3-Diphenyl-6,8-bis-(4'-*N, N*-dimethylphenylethynyl)pyrene (2e) was purified by column chromatography eluting with a 2:1 CH_2Cl_2/hexane mixture to give **2e** as a red granular solid (yield: 159 mg, 81.5%); Mp 297–298°C; ^{1}H NMR (400 MHz, $CDCl_3$): δ_H = 3.03 (s, 12H, *Me*), 6.73 (d, *J* = 8.0 Hz, 4H, Ar-*H*), 7.46–7.51 (m, 2H, Ar-*H*), 7.53–7.59 (m, 8H, Ar-*H*), 7.68 (d, *J* = 6.9 Hz, 4H, Ar-*H*), 8.00 (s, 1H, pyrene-*H*), 8.28 (d, *J* = 9.4 Hz, 2H, pyrene-*H*), 8.38 (s, 1H, pyrene-*H*), 8.64 (d, *J* = 9.4 Hz, 2H, pyrene-*H*) ppm; ^{13}C NMR (100 MHz, $CDCl_3$): δ_C = 40.2, 86.3, 96.9, 110.3, 112.0, 118.8, 125.2, 125.2, 125.8, 126.1, 127.4, 128.3, 128.4, 129.8, 130.7, 131.1, 132.7, 132.9, 138.0, 141.0, 150.3 ppm; FAB-MS: m/z calcd for $C_{48}H_{36}N_2$ 640.2878 [M^+]; found 640.2870 [M^+].

X-ray Crystallography

Suitable single crystals of **2b**, **2c** and **2e** were obtained from solution of chloroform/hexane (2:1), respectively. Diffraction data was collected at the ALS, beam line 11.3.1, using silicon 111-monochromated synchrotron radiation (λ = 0.7749 Å). Data were corrected for Lorentz and polarisation effects and for absorption from multiple and symmetry equivalent measurements.[26] The structures were solved by a charge flipping algorithm and refined by full-matrix least-squares methods on F^2.[27] For **2c** the absolute structure could not be reliably determined due to the lack of a heavy atom. In **2c** the chloroform molecule was positionally disordered over two sets of positions with major component occupancy of 62.5(5)%. There was some evidence of low occupancy second component disorder in several of the Ph and C_6H_4 rings and the OMe groups, but this was not modelled. CCDC-1812898-1812900 contain the supplementary crystallographic data for this paper. Copies of the data can be obtained, free of charge, on application to CCDC, 12 Union Road, Cambridge CB2 1EZ, UK [fax: 144-1223-336033 or e-mail: deposit@ccdc.cam.ac.uk].

Acknowledgements

This present work was performed under the Cooperative Research Program of "Network Joint Research Center for Materials and Devices (Institute for Materials Chemistry and Engineering, Kyushu University)". We would like to thank the OTEC at Saga University and the International Cooperation Projects of Guizhou Province (No. 20137002) for financial support and the EPSRC for an overseas travel grant to C.R. The Advanced Light Source is supported by the Director, Office of Science, Office of Basic Energy Sciences, of the U.S. Department of Energy under Contract No. DE-AC02-05CH11231.

Keywords: pyrene • two-photon absorption • dipolar molecule • TPA cross-section • intramolecular charge transfer

[1] a) S. Griesbeck, Z. Zhang, M. Gutmann, T. Léhmann, R. M. Edkins, G. Clermont, A. N. Lazar, M. Haehnel, K. Edkins, A. Eichhorn, M. Blanchard-Desce, L. Meinel, T. B. Marder, *Chem. - Eur. J.* **2016**, *22*, 14701−14706; b) Z. Yang, N. Zhao, Y. Sun, F. Miao, Y. Liu, X. Liu, Y. Zhang, W. Ai, G. Song, X. Shen, X. Yu, J. Sun, W. Wong, *Chem. Commun.* **2012**, *48*, 3442−3444; c) M. J. Jiang, X. G. Gu, J. W. Y. Lam, Y.L. Zhang, R. T. K. Kwok, K. S. Wong, B. Z. Tang, *Chem. Sci.* **2017**, *8*, 5440−5446.

[2] a) W. G. Fisher, W. P. Jr, Partridge, C. Dees, E. A. Wachter, *Photochem. Photobiol.* **1997**, *66*, 141−155; b) Y. Shen, A. J. Shuhendler, D. Ye, J.-J. Xu, H.-Y. Chen, *Chem. Soc. Rev.* **2016**, *45*, 6725−6741.

[3] a) S. Kawata, Y. Kawata, *Chem. Rev.* **2000**, *100*, 1777−1788; b) J. Fischer, G. von Freymann, M. Wegener, *Adv. Mater.* **2010**, *22*, 3578−3582; c) Z. Gan, Y. Cao, R. A. Evans, M. Gu, *Nat. Commun.* **2013**, *4*, 2061.

[4] a) M. Albota, D. Beljonne, J.-L. Brédas, J. E. Ehrlich, J.-Y. Fu, A. A. Heikal, S. E. Hess, T. Kogej, M. D. Levin, S. R. Marder, D. McCord-Maughon, J. W. Perry, H. Röckel, M. Rumi, G. Subramaniam, W. W. Webb, X.-L. Wu, C. Xu, *Science* **1998**, *128*, 1653−1656; b) W. R. Zipfel, R. M. Williams, W. W. Webb, *Nat. Biotechnol.* **2003**, *21*, 1369–1377; c) H. A. Collins, M. Khurana, E. H. Moriyama, A. Mariampillai, E. Dahlstedt, M. Balaz, M. K. Kuimova, M. Drobizhev, V. X. D. Yang, D. Phillips, A. Rebane, B. C. Wilson, H. L. Anderson, *Nat. Photonics* **2008**, *2*, 420−424.

[5] a) T. C. Lin,G. S. He, P. N. Prasad, L. S. Tan, *J. Mater. Chem.* **2004**, *14*, 982−991; b) L. Beverina, J. Fu, A. Leclercq, E. Zojer, P. Pacher, S. Barlow, E. W. Van Stryland,D. J. Hagan, J. L. Bredas, S. R. Marder, *J. Am. Chem. Soc.* **2005**, *127*, 7282−7283; c) C. L. Sun, Q. Liao, T. Li, J. Li, J. Q. Jiang, Z. Z. Xu, X. D. Wang, R. Shen, D. C. Bai, Q. Wang, S. X. Zhang, H. B. Fu, H. L. Zhang, *Chem. Sci.* **2015**, *6*, 761−769.

[6] a) M. Rumi, J. E. Ehrlich, A. A. Heikal, J. W. Perry, S. Barlow, Z. Y. Hu, D. McCord-Maughon, T. C. Parker, H. Rockel, S. Thayumanavan, S. R. Marder, D. Beljonne, J. L. Bredas, *J. Am. Chem. Soc.* **2000**, *122*, 9500−9510; b) O. Mongin, L. Porrès, M. Charlot, C. Katan, M. Blanchard-Desce, *Chem. - Eur. J.* **2007**, *13*, 1481−1498.

[7] a) Y. H. Jiang, Y. C. Wang, J. L. Hua, J. Tang, B. Li, S. X. Qian, H. Tian, *Chem. Commun.* **2010**, *46*, 4689−4691; b) J. Shao, Z. Guan, Y. Yan, C. Jiao, Q.-X. Xu, C. Chi, *J. Org. Chem.* **2011**,

76, 780−790; c) Y. M. Poronik, V. Hugues, M. Blanchard-Desce, D. T. Gryko, *Chem. - Eur. J.* **2012**, *18*, 9258−9266.
[8] a) G. S. He, J. Swiatkiewicz, Y. Jiang, P. N. Prasad, B. A. Reinhardt, L. S. Tan, R. Kannan, *J. Phys. Chem. A* **2000**, *104*, 4805–4810; b) M. M. Alam, M. Chattopadhyaya, S. Chakrabarti, K. Ruud, *Acc. Chem. Res.* **2014**, *47*, 1604−1612; c) B. Dereka, M. Koch, E. Vauthey, *Acc. Chem. Res.* **2017**, *50*, 426−434.
[9] D. Jérome, H. J. Schulz, *Advances in Physics*, **2002**, *51*, 293−479.
[10] a) T. M. Figueira-Duarte, K. Müllen, *Chem. Rev.* **2011**, *111*, 7260–7314; b) X. Feng, J. Y. Hu, C. Redshaw, T. Yamato, *Chem. - Eur. J.* **2016**, *22*, 11898–11916.
[11] a) H. M. Kim, Y. O. Lee, C. S. Lim, J. S. Kim, B. R. Cho, *J. Org. Chem.* **2008**, *73*, 5127–5130; b) J. Sung, P. Kim, Y. O. Lee, J. S. Kim, D. Kim, *J. Phys. Chem. Lett.* **2011**, *2*, 818–823; c) Y. Niko, H. Moritomo, H. Sugihara, Y. Suzuki, J. Kawamata, G. Konishi, *J. Mater. Chem. B* **2015**, *3*, 184–190; d) C. L. Devi, K. Yesudas, N. S. Makarov, V. J. Rao, K. Bhanuprakash, J. W. Perry, *J. Mater. Chem. C* **2015**, *3*, 3730—3744; e) M. Gascón-Moya, A. Pejoan, M. Izquierdo-Serra, S. Pittolo, G. Cabré, J. Hernando, R. Alibés, P. Gorostiza, F. Busqué, *J. Org. Chem.* **2015**, *80*, 9915−9925; f) S. Lee, D. Kim, *J. Phys. Chem. A* **2016**, 120, 9217–9223.
[12] a) Y. Wan, L. Yan, Z. Zhao, X. Ma, Q. Guo, M. Jia, P. Lu, G. Ramos-Ortiz, J. L. Maldonado, M. Rodríguez, A. Xia, *J. Phys. Chem. B* **2010**, *114*, 11737–11745; b) P. L. Burn, S. C. Lo, I. D. W. Samuel, *AdV. Mater.* **2007**, *19*, 1675–1688.
[13] a) L. Zöphel, V. Enkelmann, K. Müllen, *Org. Lett.* **2013**, *15*, 804–807; b) X. Feng, H. Tomiyasu, J. Y. Hu, X. F. Wei, C. Redshaw, M. R. J. Elsegood, L. Horsburgh, S. J. Teat, T. Yamato, *J. Org. Chem.* **2015**, *80*, 10973–10978; c) Y. Niko, S. Sasaki, K. Narushima, D. K. Sharma, M. Vacha, G.-i. Konishi, *J. Org. Chem.* **2015**, *80*, 10794−10805; d) C. Z. Wang, H. Ichiyanagi, K. Sakaguchi, X. Feng, M. R. J. Elsegood, C. Redshaw, T. Yamato, *J. Org. Chem.* **2017**, *82*, 7176−7182; e) C. Z. Wang, X. Feng, Z. Kowser, C. Wu, T. Akther, M. R.J. Elsegood, C. Redshaw, T. Yamato, *Dyes Pigments* **2018**, *153*, 125–131; f) C. Z. Wang, Y. Noda, C. Wu, X. Feng, P. Venkatesan, H. Cong, M. R. J. Elsegood, T. G. Warwick, S. J. Teat, C. Redshaw, T. Yamato, *Asian J. Org. Chem.* **2018**, *7*, 444–450.
[14] a) K. Shizu, H, Tanaka, M. Uejima, T. Sato, K. Tanaka, H. Kaji, C. Adachi, *J. Phys. Chem. C* **2015**, *119*, 1291−1297; b) P. Rajamalli, N. Senthilkumar, P. Gandeepan, P. Y. Huang, M. J. Huang, C. Z. RenWu, C. Y. Yang, M. J. Chiu, L. K. Chu, H. W. Lin, C. H. Cheng, *J. Am. Chem. Soc.* **2016**, *138*, 628−634.
[15] M. A. Albota, C. Xu, W. W. Webb, *Appl. Opt.* **1998**, *37*, 7352−7356.
[16] a) V. E. Lippert, Z. *Naturforsch, A: Phys. Sci.* **1955**, *10*, 541−545; b) N, Mataga, Y. Kaifu, M, Koizumi, *Bull. Chem. Soc. Jpn.* **1956**, *29*, 465−470.
[17] a) T. Jadhav, B. Dhokale, Y. Patil, S. M. Mobin, R. Misra, *J. Phys. Chem. C* **2016**, *120*, 24030−24040; b) R. P. Tayade, N. Sekar, *J. Lumin.* **2016**, *176*, 298−308; c) C.-H. Lim, M. D. Ryan, B. G. McCarthy, J. C. Theriot, S. M. Sartor, N. H. Damrauer, C. B. Musgrave, G. M. Miyake, *J. Am. Chem. Soc.* **2017**, *139*, 348−355.
[18] H. N. Zhu, X. Wang, R. J. Ma, Z. R. Kuang, Q. J. Guo, A. D. Xia, *ChemPhysChem* **2016**, *17*, 3245–3251.
[19] a) M. Sheik-Bahae, A. A. Said, T.-H. Wei, D. G. Hagan, E. W. van Stryland, *IEEE J. Quantum Electron.* **1990**, *26*, 760−769; b) K. Kamada, K. Matsunaga, A. Yoshino, K. Ohta, *J. Opt. Soc. Am. B* **2003**, *20*, 529−537.
[20] C. Xu, W. W. Webb, *J. Opt. Soc. Am. B* **1996**, *13*, 481–491.
[21] J. N. Demas, G. A. Crosby, *J. Phys. Chem.* **1971**, *75*, 991–1024.
[22] a) Z. F. Chang, L. M. Jing, B. Chen, M. Zhang, X. Cai, J. J. Liu, Y. C. Ye, X. Lou, Z. Zhao, B. Liu, J. L. Wang, B. Z. Tang, *Chem. Sci.* **2016**, *7*, 4527–4536; b) J. Tian, J. Zhang, W. Li, L. Q. Zhang, D. M. Yue, *J. Mater. Chem. C* **2016**, *4*, 10146–10153; c) A. X. Ding, H. J. Hao, Y. G. Gao, Y. D. Shi, Q. Tang, Z. L. Lu, *J. Mater. Chem. C* **2016**, *4*, 5379–5389.
[23] a) (a) Y. Q. Xu, Q. Chen, C. F. Zhang, R. Wang, H. Wu, X. Y. Zhang, G. C. Xing, W. W. Yu, X. Y. Wang, Y. Zhang, M. Xiao, *J. Am. Chem. Soc.* **2016**, *138*, 3761−3768; b) Q. J. Han, W. Z. Wu, W. L. Liu, Y. Q. Yang, *RSC Adv.* **2017**, *7*, 35757−35764.
[24] Y. Wang, X. M. Li, X. Zhao, L. Xiao, H. B. Zeng, H. D. Sun, *Nano. Lett.* **2016**, *16*, 448–453.
[25] a) Z. Q. Liu, Q. Fang, D. Wang, D. X. Cao, G. Xue, W. T. Yu, H. Lei, *Chem. Eur. J.* **2003**, *9*, 5074–5084; b) J. Chen, P. Chábera, T. Pascher, M. E. Messing, R. Schaller, S. Canton, K. Zheng, T. Pullerits, *J. Phys. Chem. Lett.* **2017**, *8*, 5119–5124.
[26] APEX 2 & SAINT (2012), software for CCD diffractometers. Bruker AXS Inc., Madison, USA.
[27] a) G. M. Sheldrick, *Acta Crystallogr.* **2008**, *A64*, 112–122; b) G. M. Sheldrick, *Acta Cryst.* **2015**, *A71*, 3–8; c) G. M. Sheldrick, *Acta Cryst.* **2015**, *C71*, 3–8.

Entry for the Table of Contents (Please choose one layout)

Layout 2:

FULL PAPER

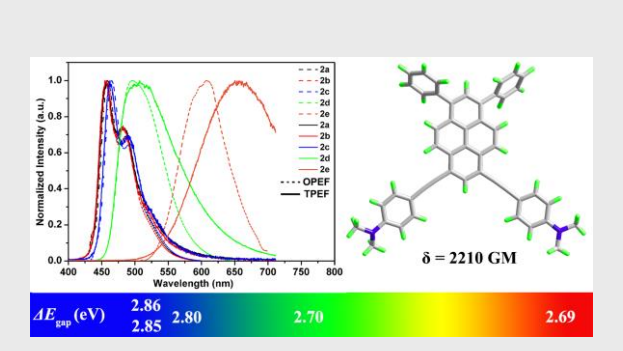

Chuan-Zeng Wang,[a] Ruoyao Zhang,[b] Koya Sakaguchi,[a] Xing Feng,[c] Xiaoqiang Yu,[b] Mark R.J. Elsegood,[d] Simon J. Teat,[e] Carl Redshaw,[f] and Takehiko Yamato*[a]*

Page No. – Page No.

Two-Photon Absorption Properties of Pyrene-based Dipolar D–π–A Fluorophores

CIF

[checkCIF Results]

Manuscript number: cptc.201800053
MS Type: Article
Title: "Two-Photon Absorption Properties of Pyrene-based Dipolar D-π-A Fluorophores"
Correspondence Author: Prof. Dr. Takehiko Yamato
****

Dear Prof. Dr. Deanne Nolan,

On behalf of my co-authors, we thank you very much for your review content. We have studied reviewer's comments carefully and have made revision which marked in yellow in the manuscript. We would like to submit for your kind consideration.

****

COMMENTS TO AUTHOR:

Reviewer 1: The revisions that the authors have made are satisfactory and quite consistent with previous works. But I still suggest that the authors should include the following two appropriate papers

(J. Phys. Chem. A 2016, 120, 9217-9223, J. Phys. Chem. Lett. 2011, 2, 818-823) in the reference.

Response: According to referee's suggestion, we have cited these two papers in the revised manuscript.

Reviewer 2: The manuscript is improved from its original submission, but there are a few issues that can be resolved prior to publication.

P4Col2L7-11. The sentence that compares the EWG and EDG effects of 2a to 2b and 2c is confusing. In a pi-conjugated system that is connected through resonance, OMe is commonly an EDG, why is OMe described as an EWG here. Their DFT results suggest 2c (OMe) has a higher HOMO (donor) than 2a and a higher LUMO than 2a.

What about TD-DFT?

Response: Thank you very much for your most perceptive review. We have improved this

part in the revised manuscript. We regret for the lack of the TD-DFT results, because of the lower performance of our computer. Generally, we just provide as much evidence as possible to explain the properties with the aid of the DFT calculations. I sincerely hope that you will satisfied with the current results, anyhow, current DFT results are quite consistent with the photophysical properties.

Structure 2 in Scheme 1 should be re-drawn to show double bonds in pyrene adopting a biphenyl structure. The central double bond should switch position.

Response: Thank you very much for your suggestion. We have improved this part in the revised version.

The authors are standing firm that the reported molar absorptivites are accurate to 5 significant figures, thus I request a Beer-Lambert plot of several concentrations in the SI to support this high accuracy.

Response: Thank you very much for your suggestion. I am so sorry we misunderstood referee's suggestion previously. We also think our accuracy is unreasonable because of the numerous source of error. So we improved the significant figures in the revised version.

Please include the R2 values in the Lippert-Mataga plots.

Response: According to referee's suggestion, we have added the R2 values in the revised manuscript. Although the linearity is not ideal, nearly linear fits can still provide increasing trend from 2a to 2e.

The abstract still contains meaningless structure numbers, such as 2e, please revise.

Response: According to referee's suggestion, we have improved this issue in the revised manuscript.

The experimental section still lists silica gel in millimeter diameter, which I believe is incorrect and should be micrometer.

Response: Thank you very much for your suggestion. We have checked the label of our silica gel carefully, they provide the detailed information in millimeter diameter.

The synthesis section should be re-ordered to start at 2a and proceed to 2e. There is still a labelled negative direction peak in the 13C NMR of 2b and 2d? Why? Also, the authors need to verify the number of 13C peaks - are each of the unique carbons accounted for in the characterization list?

Response: According to referee's suggestion, we have remeasured ^{13}C NMR of 2b and 2d, and we also re-ordered the synthesis section in the revised manuscript.

The accuracy of the HR-MS results are astonishing - each actual mass matches the theoretical mass to 4 decimals, not only here but also in a prior publication 13e. This reviewer needs to see the raw analytical data set to confirm the accuracy.

Response: Thank you very much for your suggestion. we checked the original data of HR-MS carefully, we made a mistake, we have improved the MS results and added the original spectra (Figures S18-27) in the revised manuscript.

Figure S14 of the SI are not PL intensity, but rather absorption spectra.

Response: Thank you very much for your carefully review, we have corrected the absorption spectra.

Clearly, some references have been added to citation 13 and of particular note is 13e, their own work in Dyes&Pigments. Given the submission/acceptance dates, 13e is very related to the work here (without 2PA). The main difference between the two manuscripts is 13e contains a

t-butyl group in position 7. This minor difference in structure is concerning for two reasons. First, it could indicate unnecessary dilution of publication quality. Second, why is the published work from 13e not explicitly used as comparator data in this manuscript?

Response: Thank you very much for your most perceptive review. Actually, the published work of reference 13e is the other work of our group, although the differences of these two work present in the position and substituent (*tert*-butyl), the properties display significant difference. Such as two-photon absorption properties, photosensitivity versus position and substituents, thermostability. The underlying mechanisms was not well understood. What is more, our group have already prepared some new pyrene-based D-π-A molecules with wide visible emission (such as 1,3-Acceptor-6,8-Donor pyrene, 1,3-Acceptor-5,9-Donor-tert-butyl pyrene, 1-Donor-3-Acceptor-7-tert-butyl pyrene etc), and that new results will release soon. Then, we will make a systematic summary for the work mechanisms according to the experimental and theoretical works as much as possible.

Once these concerns are address, I feel the manuscript is acceptable.

Hopefully we have addressed the reviewer's concerns.

Two-Photon Absorption Properties of Pyrene-based Bipolar D–π–A Fluorophores

Chuan-Zeng Wang,[a] Ruoyao Zhang,[b] Koya Sakaguchi,[a] Xing Feng,*[c] Xiaoqiang Yu,[b] Mark R.J. Elsegood,[d] Simon J. Teat,[e] Carl Redshaw,[f] and Takehiko Yamato*[a]

Rational design of pyrene-based dipolar molecules with large two-photon absorption cross section (δ) and efficient two-photon brightness ($\delta\Phi$) was reported aided by the theoretical calculations.